ICHEP94 Ref. GSL0156
Submitted to Pa 16 Pl 9

CLEO CONF 94-21
July 18, 1994

# $\pi^-\pi^+$ Energy Correlation in $\tau$ Pair Events.

J. Bartelt,[1] S.E. Csorna,[1] Z. Egyed,[1] V. Jain,[1] D. Gibaut,[2] K. Kinoshita,[2] P. Pomianowski,[2] B. Barish,[3] M. Chadha,[3] S. Chan,[3] D.F. Cowen,[3] G. Eigen,[3] J.S. Miller,[3] C. O'Grady,[3] J. Urheim,[3] A.J. Weinstein,[3] M. Athanas,[4] W. Brower,[4] G. Masek,[4] H.P. Paar,[4] M. Sivertz,[4] J. Gronberg,[5] R. Kutschke,[5] S. Menary,[5] R.J. Morrison,[5] S. Nakanishi,[5] H.N. Nelson,[5] T.K. Nelson,[5] C. Qiao,[5] J.D. Richman,[5] A. Ryd,[5] D. Sperka,[5] H. Tajima,[5] M.S. Witherell,[5] R. Balest,[6] K. Cho,[6] W.T. Ford,[6] D.R. Johnson,[6] K. Lingel,[6] M. Lohner,[6] P. Rankin,[6] J.G. Smith,[6] J.P. Alexander,[7] C. Bebek,[7] K. Berkelman,[7] K. Bloom,[7] T.E. Browder,[7*] D.G. Cassel,[7] H.A. Cho,[7] D.M. Coffman,[7] D.S. Crowcroft,[7] P.S. Drell,[7] D. Dumas,[7] R. Ehrlich,[7] P. Gaidarev,[7] R.S. Galik,[7] M. Garcia-Sciveres,[7] B. Geiser,[7] B. Gittelman,[7] S.W. Gray,[7] D.L. Hartill,[7] B.K. Heltsley,[7] S. Henderson,[7] C.D. Jones,[7] S.L. Jones,[7] J. Kandaswamy,[7] N. Katayama,[7] P.C. Kim,[7] D.L. Kreinick,[7] G.S. Ludwig,[7] J. Masui,[7] J. Mevissen,[7] N.B. Mistry,[7] C.R. Ng,[7] E. Nordberg,[7] J.R. Patterson,[7] D. Peterson,[7] D. Riley,[7] S. Salman,[7] M. Sapper,[7] F. Würthwein,[7] P. Avery,[8] A. Freyberger,[8] J. Rodriguez,[8] S. Yang,[8] J. Yelton,[8] D. Cinabro,[9] T. Liu,[9] M. Saulnier,[9] R. Wilson,[9] H. Yamamoto,[9] T. Bergfeld,[10] B.I. Eisenstein,[10] G. Gollin,[10] B. Ong,[10] M. Palmer,[10] M. Selen,[10] J. J. Thaler,[10] K.W. Edwards,[11] M. Ogg,[11] A. Bellerive,[12] D.I. Britton,[12] E.R.F. Hyatt,[12] D.B. MacFarlane,[12] P.M. Patel,[12] B. Spaan,[12] A.J. Sadoff,[13] R. Ammar,[14] P. Baringer,[14] A. Bean,[14] D. Besson,[14] D. Coppage,[14] N. Copty,[14] R. Davis,[14] N. Hancock,[14] M. Kelly,[14] S. Kotov,[14] I. Kravchenko,[14] N. Kwak,[14] H. Lam,[14] Y. Kubota,[15] M. Lattery,[15] M. Momayezi,[15] J.K. Nelson,[15] S. Patton,[15] R. Poling,[15] V. Savinov,[15] S. Schrenk,[15] R. Wang,[15] M.S. Alam,[16] I.J. Kim,[16] Z. Ling,[16] A.H. Mahmood,[16] J.J. O'Neill,[16] H. Severini,[16] C.R. Sun,[16] F. Wappler,[16] G. Crawford,[17] C. M. Daubenmier,[17] R. Fulton,[17] D. Fujino,[17] K.K. Gan,[17] K. Honscheid,[17] H. Kagan,[17] R. Kass,[17] J. Lee,[17] R. Malchow,[17] M. Sung,[17] C. White,[17] M.M. Zoeller,[17] F. Butler,[18] X. Fu,[18] B. Nemati,[18] W.R. Ross,[18] P. Skubic,[18] M. Wood,[18] M. Bishai,[19] J. Fast,[19] E. Gerndt,[19] R.L. McIlwain,[19] T. Miao,[19] D.H. Miller,[19] M. Modesitt,[19] D. Payne,[19] E.I. Shibata,[19] I.P.J. Shipsey,[19] P.N. Wang,[19] M. Battle,[20] J. Ernst,[20] L. Gibbons,[20] Y. Kwon,[20] S. Roberts,[20] E.H. Thorndike,[20] C.H. Wang,[20] J. Dominick,[21] M. Lambrecht,[21] S. Sanghera,[21] V. Shelkov,[21] T. Skwarnicki,[21] R. Stroynowski,[21] I. Volobouev,[21] G. Wei,[21] P. Zadorozhny,[21] M. Artuso,[22] M. Gao,[22] M. Goldberg,[22] D. He,[22] N. Horwitz,[22] G.C. Moneti,[22] R. Mountain,[22] F. Muheim,[22] Y. Mukhin,[22] S. Playfer,[22] Y. Rozen,[22] S. Stone,[22] X. Xing,[22] and G. Zhu[22]

(CLEO Collaboration)

[1] *Vanderbilt University, Nashville, Tennessee 37235*
[2] *Virginia Polytechnic Institute and State University, Blacksburg, Virginia, 24061*
[3] *California Institute of Technology, Pasadena, California 91125*
[4] *University of California, San Diego, La Jolla, California 92093*
[5] *University of California, Santa Barbara, California 93106*
[6] *University of Colorado, Boulder, Colorado 80309-0390*
[7] *Cornell University, Ithaca, New York 14853*
[8] *University of Florida, Gainesville, Florida 32611*
[9] *Harvard University, Cambridge, Massachusetts 02138*
[10] *University of Illinois, Champaign-Urbana, Illinois, 61801*
[11] *Carleton University, Ottawa, Ontario K1S 5B6 and the Institute of Particle Physics, Canada*
[12] *McGill University, Montréal, Québec H3A 2T8 and the Institute of Particle Physics, Canada*
[13] *Ithaca College, Ithaca, New York 14850*
[14] *University of Kansas, Lawrence, Kansas 66045*
[15] *University of Minnesota, Minneapolis, Minnesota 55455*
[16] *State University of New York at Albany, Albany, New York 12222*
[17] *Ohio State University, Columbus, Ohio, 43210*
[18] *University of Oklahoma, Norman, Oklahoma 73019*
[19] *Purdue University, West Lafayette, Indiana 47907*
[20] *University of Rochester, Rochester, New York 14627*
[21] *Southern Methodist University, Dallas, Texas 75275*
[22] *Syracuse University, Syracuse, New York 13244*

## Abstract

We report on a measurement of the magnitude of the tau neutrino helicity $|h_\nu|$ from $\tau^+\tau^-$ events taken with the CLEO II detector at the CESR $e^+e^-$ storage ring. Events in which both taus decay into a charged pion and a neutrino are analyzed for energy correlations between the daughter pions, yielding $|h_\nu|$=0.99 $\pm$ 0.06 $\pm$ 0.10, where the first error is statistical and the second systematic.

---

*Permanent address: University of Hawaii at Manoa

In the Standard Model of particle physics there are three neutrinos, $\nu_e, \nu_\mu, \nu_\tau$, which belong to left-handed weak isodoublets without a corresponding right-handed singlet; *i.e.*, the neutrinos are left-handed leptons, tau decay is a V-A process, and the $\nu_\tau$ helicity is $h_\nu = -1$. [1] In the rest frame of a $\tau^{-(+)}$ that decays to $\pi\nu$, the parent spin is maximally correlated (anticorrelated) to the daughter meson direction. Tau pairs have preferentially aligned spins when produced via the QED process $e^+e^- \rightarrow \gamma^* \rightarrow \tau^+\tau^-$. At center-of-mass energies above $\tau^+\tau^-$ threshold, each $\tau$ has a relativistic boost, and the meson directions in the center-of-mass systems are partially Lorentz-transformed into hadron energies. Thus for a left-handed $\nu_\tau$, the energies of the $\pi^+$ and the $\pi^-$ are correlated. This correlation is also present if $\nu_\tau$ was instead right handed with $h_\nu = +1$. However, if $\nu_\tau$ has no preferred handedness there will be no correlations between the daughter energies. The energy correlations in this process are thus not explicitly parity violating, but are nonetheless a consequence of parity violation in $\tau$ decays.

In this Contribution we report on the first measurement of $|h_\nu|$ using the energy-energy correlations in the final state $(\pi^+\overline{\nu})(\pi^-\nu)$ at center-of-mass energies of $\sqrt{s} = 10.6$ GeV. A recent measurement by ARGUS [2] at this energy used the $(\rho^+\overline{\nu})(\rho^-\nu)$ final state and a study by ALEPH [3] involved both $(\pi^+\overline{\nu})(\pi^-\nu)$ and $(\rho^+\overline{\nu})(\rho^-\nu)$ at $\sqrt{s} = m_Z$. An ARGUS measurement [4] of asymmetries in three-pion decays of the $\tau$ has unambiguously determined the sign of $h_\nu$ as negative.

For the decay of the $\tau$ to a pseudoscalar (*e.g.*, $\pi$) the neutrino helicity $h_\nu$ is related to to the parameters $\gamma_{av}$ and $\xi$ and the charged current couplings $g_a$ and $g_v$ by [5–7]

$$h_\nu = \xi_\pi = -\gamma_{av} = \frac{-2g_a g_v}{g_a^2 + g_v^2}.$$

The double differential cross section in the laboratory energies of the hadrons is given by

$$\frac{d^2\sigma}{dE_+ dE_-} = F_1(E_+, E_-) + h_\nu^2 \cdot F_2(E_+, E_-),$$

with $F_1$ and $F_2$ being known kinematic functions. As noted above, the measurement of this correlation cannot determine the sign of the neutrino helicity, only the magnitude. For either $V - A$ or $V + A$ interactions the correlations will be maximal, whereas for pure $V$ or pure $A$ interactions the correlations will vanish.

The strategy employed is as follows:

(i) Extract $\tau^+\tau^- \rightarrow (\pi^+\overline{\nu})(\pi^-\nu)$ events from the data that are relatively free of backgrounds from non-tau processes;

(ii) Generate samples of simulated events for $V$ and $V - A$ interactions, mixing them appropriately to obtain a desired value of $|h_\nu|$;

(iii) Using a likelihood method, determine what value of $h_\nu$ best matches the data;

(iv) Carefully evaluate the techniques and selection criteria for possible systematic biases.

The data were taken at the Cornell Electron Storage Ring (CESR) with the CLEO II detector. [8] Drift chambers in a 1.5 T axial magnetic field provide charged particle tracking with momentum resolution $\sigma_p/p(\%) \simeq \sqrt{(0.15p)^2 + (0.5)^2}$, $p$ in GeV/$c$. These chambers occupy the radius 4.7 to 90 cm. The innermost chamber is a 6-layer straw-tube device, followed by a 10-layer pressurized wire vertex chamber and a 51-layer main drift chamber. The z-coordinates of a track are measured using the 11 stereo layers of the main drift chamber and 4 segmented cathode planes, which are located at the inner and outer radii of the wire vertex detector and the main drift chamber. Outside these chambers are plastic scintillator counters that measure time-of flight and also act as primary inputs to the trigger.

The CLEO II electromagnetic calorimeter is an array of 7800 CsI(Tl) crystals, divided into a barrel region and two endcaps. The 6144 barrel crystals, arranged in a projective geometry, surround the tracking chambers and time-of-flight system at $\sim$1 m radius, covering $|\cos\theta| < 0.82$, with $\theta$ the polar angle with respect to the beam direction. Two identical endcaps, each composed of 828 rectangular crystals, extend the hermetic solid angle coverage to the region $0.80 < |\cos\theta| < 0.98$. The barrel calorimeter achieves energy and angular resolutions $\sigma_E/E(\%) = 0.35/E^{0.75} + 1.9 - 0.1E$, $\sigma_\phi(\text{mrad}) = 2.8/\sqrt{E} + 1.9$, and $\sigma_\theta(\text{mrad}) = 0.8\sigma_\phi \sin\theta$, $E$ in GeV.

To achieve muon identification, three layers of 36 cm thick iron absorbers are arranged in an octagonal geometry to surround the superconducting magnet coil and the iron pole pieces of the magnet. Proportional counters instrument the two gaps between the iron pieces and the exterior of the third layer, with additional counters covering the endcap region.

A three-tier hardware trigger system takes input from the calorimeter, tracking chambers, and scintillation counters to form different combinations of requirements that force readout of the detector. [9] A fourth level filter in software uses information from the entire detector to reject about half of the hardware triggers.

The data set corresponds to 1.64 fb$^{-1}$ of luminosity taken on and slightly below the $\Upsilon(4S)$ resonance, at center-of-mass energies of $\sqrt{s} = 2E_{\text{bm}} \simeq 10.6$ GeV. This corresponds to roughly 1.5 million $\tau^+\tau^-$ events produced in the detector. Since not all the data is at one value of $E_{\text{bm}}$, this analysis uses the scaled track energy, $x = \sqrt{p^2 + m_\pi^2}$ instead of $E_\pi$.

Events are first selected that have exactly two charged tracks which are in the fiducial volume of the tracking system, and have (i) opposite charge, (ii) $|\cos(\theta)| < 0.7$, (iii) $x > 0.2$ and (iv) projections consistent with coming from the nominal event vertex.

To reduce the contamination of non-$\tau\tau$ QED events, we demand at most one track have $x > 0.8$, that the total shower energy in the electromagnetic calorimeter be less that $0.85\sqrt{s}$. To remove backgrounds from final states that involve electrons, each track must have its electromagnetic calorimeter energy be less than 85% of its momentum as measured in the tracking chambers. These criteria reduce the number of events to about 115,000.

Further criteria are applied to reduce the backgrounds from $\gamma\gamma$ induced reactions, to remove as many muons from the sample as possible, and to deplete the feed-down from higher mass final states containing neutral pions. The most effective variable for removing the two-photon events is $\theta_{\text{min}}$ which is defined as

$$\sin\theta_{\text{min}} = \frac{|\vec{p}_\perp|}{E_{bm} \cdot (2 - x_- - x_+)},$$

*i.e.*, the ratio of the missing net momentum transverse to the beams to the missing energy of the event. In Fig. 1 we show the distribution of this variable for simulated $\gamma\gamma$ events that have two hadrons in the detector and $\pi\pi$ final states from $\tau^+\tau^-$ events. In addition, at least one of the tracks is required to have $x > 0.3$.

Final states that contain neutral pions are suppressed by demanding no isolated showers in the calorimeter. These are showers in the calorimeter not matched to charged tracks and that are in excess of 50(350) MeV if they are outside(inside) a cone about the charged track with half angle $\cos^{-1}(0.97)$. Fig. 2 shows the agreement of data and simulation for this criteria in lepton *vs.* $\rho$ final states and indicates an efficiency of roughly 85% per track over the entire momentum range.

Discrimination against muons involves four independent criteria, three of which use information from the muon chambers and the charged track projection and one of which demands the particle leave an energy deposition in the calorimeter that is inconsistent with that of a muon; each track must pass one of these four criteria for the event to be accepted. The efficiency of these criteria to select a track as a pion has been measured using an independent sample of identified pions; it has a threshold at $x \sim 0.2$, rises sharply to 55% at $x \sim 0.25$, and reaches a plateau of about 65% by $x \sim 0.5$. Studies of radiative mu-pair events in both data and simulation indicate a fake rate of less than 2% per track over the kinematic range of this analysis.

Finally a restriction was imposed to minimize possible systematic effects from triggering. Over the course of the data collection the requirements of the hardware trigger had been made less stringent; events were kept only if the trigger information showed they would have passed the most rigorous of the requirements.

These events are binned in $x_+$ *vs.* $x_-$ with bin size 0.1 and range $0.2 < x_\pm < 0.95$ as shown in Fig. 3. The number of data events in each of the 59 bins is denoted as $d_{ij}$, with $i$ and $j$ indexing the bin. This figure clearly shows the depletion in the corners that have one energetic and one slow hadron, as expected for $V \pm A$. We are left with 1972 candidates from which to extract $|h_\nu|$.

The Monte Carlo simulations start with the KORALB [10] $\tau$ generator and use the GEANT package [11] to model the CLEO II detector. A large sample of $\tau^+\tau^-$ events were generated to assess which decay modes were significant sources of background for the analysis. It was found that 97% of all such events that passed the selection criteria came from the five final states involving $\pi\pi$, $\pi K$, $\pi\rho$, $\pi\mu$, and $\pi K^*$. Samples corresponding to several times the actual data are then generated for these five modes both with the $V - A$ and with the $V$ hypotheses. The results are scaled to the 1.64 fb$^{-1}$ of luminosity and binned as $x_+$ *vs.* $x_-$. For each bin $(i,j)$ the predicted number of events, denoted $n_{ij}$ for *any* value of $h_\nu$ is given by [12]

$$n_{ij}(h_\nu) = h_\nu^2 \cdot N_{ij}^{V-A} + (1 - h_\nu^2) \cdot N_{ij}^{V}.$$

A binned Poisson likelihood is then taken as a function of $h_\nu$ as

$$\log \mathcal{L}(h_\nu) = \sum_{i,j} [d_{ij} \log n_{ij} - n_{ij} - \log(d_{ij}!)].$$

The result is shown in Fig. 4 and gives

$$|h_\nu| = 0.99 \pm 0.06,$$

with the uncertainty being statistical. Note that the normalization in this expression comes entirely from the simulation. If the normalization is incorporated in the fitting procedure the result changes to $|h_\nu| = 1.00$. We have also used a $\chi^2$ analysis to analyze the data as a check. Since the values of $d_{ij}$ are not large in some bins, we have doubled the bin width in each dimension, leading to 15 bins for the $\chi^2$ analysis. The result is $|h_\nu| = 1.03 \pm 0.08$ if the normalization is fixed to that of the simulation and $|h_\nu| = 1.04 \pm 0.08$ if it is allowed to be determined by the fit; the goodness of the fits, as measured by $\chi^2$/d.f., are 12.2/14 and 9.8/13, respectively. Fig. 5 shows the distribution of $\Delta_{ij} = (d_{ij} - n_{ij})/\sqrt{n_{ij}}$ across the $x_+$ versus $x_-$ plane for the best fit value of $h_\nu$. White boxes denote positive values and black poxes, negative. The distribution of the 59 $\Delta_{ij}$ values are well described by a Gaussian of mean 0.09 and width 1.00.

We have made many systematic checks which can be divided into four broad categories: (i) dependence on the values of variables used in event selection, (ii) possible biases in the methodology, (iii) possible biases in the simulations, and (iv) our estimate of backgrounds.

The kinematic and fiducial requirements are standard for low-multiplicity analyses and have been assigned, based on variations of the criteria, an uncertainty of $\delta|h_\nu| = 0.02$. As an example we show in Fig. 6 the scaled momentum spectrum for the charged pions in the data, in the simulation events in the $\pi\pi$ final state, and the generic $\tau^+\tau^-$ simulation; the agreement is excellent. We have varied the limit on $\sin\theta_{\rm min}$ and tried replacing the criterion altogether with a higher limit on the minimum pion energies; these result in an estimate of $\delta|h_\nu| = 0.02$. Similarly the energies and angles associated with the removal of isolated showers were varied, changing the acceptance by roughly 10%, and indicating a possible systematic uncertainty of $\delta|h_\nu| = 0.03$. Somewhat larger variations in $|h_\nu|$ were observed when changing the hadron/muon criteria. Subsets of the four exclusive criteria were tried, resulting in acceptance variations of up to 75%; the magnitude and shape parameters of the shower requirement in the calorimeter were also varied, as was the fiducial volume of the muon chambers. From these an estimate of $\delta|h_\nu| = 0.05$ was obtained. To check possible biases in the trigger requirements, three variations were tried: portions of the data set were analyzed with the (looser) trigger with which they were taken; the simulation was run without any trigger requirement; an additional requirement on energy balance for positive and negative $\cos\theta$ was imposed. These indicate a maximal bias of $\delta|h_\nu| = 0.03$.

A large sample of $\tau^+\tau^-$ simulation events were generated with all known decay modes [13] under the $V - A$ hypothesis. These are the samples used for other CLEO II $\tau$ analyses. Simulated events form the various running conditions were formed into three statistically independent samples, each corresponding to 1.64 fb$^{-1}$ of data collection. The analysis then was run on each of these simulated data sets. The results are consistent with that from the data within an uncertainty of $\delta|h_\nu| = 0.04$. As previously mentioned we can allow the normalization to be determined by the fitting procedure instead of by the simulation, leading to $\delta|h_\nu| = 0.01$. From the parallel $\chi^2$ analysis we assign a further possible systematic error for the likelihood technique of $\delta|h_\nu| = 0.03$.

Three of the criteria used in event selection (hadron identification, removal of events with isolated calorimeter showers, and efficiency of the calorimeter trigger) have been evaluated using a clean sample of identified pions from $\tau^+\tau^-$ events with the lepton *vs.* $\rho$ decay topology. One of these was shown in Fig. 2. The simulation was used in the analysis due to the lack of data events with high hadron $x$. Using the data instead for these efficiencies makes very minor changes in the result and we estimate $\delta|h_\nu| = 0.02$ as a systematic error contribution. Since the vast majority of the events involve one or more charged pions, the value of the branching fraction $B_\pi$ was varied, resulting in variations of $\delta|h_\nu| = 0.03$.

Possible uncertainties in the backgrounds induced by $\gamma\gamma$ interaction were already accounted for in our variation of the criteria involving $\sin\theta$. Similarly, background variations from the most dominant $\tau$ backgrounds, those involving a $\rho$ in the final state, were addressed by the checks on the isolated shower criteria. To assess the possible contamination from $\mu\mu\gamma$ final states, we took events of this type, assigned a fake rate per track of 5% (*double* the measured value), added these to the general $V-A$ $\tau^+\tau^-$ simulation, and re-evaluated $|h_\nu|$, obtaining a shift of 0.02. We therefore assign $\delta|h_\nu| = 0.01$ for possible effects from this background.

The systematic errors are summarized in the Table below. Taking all the effects in quadrature we obtain an overall systematic uncertainty of $\delta|h_\nu| = \pm 0.10$.

| Parameter | $\Delta\xi$ |
|---|---|
| Kinematic criteria | 0.02 |
| $\gamma\gamma$ veto | 0.02 |
| Isolated shower veto | 0.03 |
| Hadron identification | 0.05 |
| Trigger and `LEVEL3` | 0.03 |
| Simulation comparisons | 0.04 |
| Normalizations | 0.01 |
| $\log\mathcal{L}$ vs $\chi^2$ | 0.04 |
| Data-based corrections | 0.03 |
| Tau branching ratios | 0.03 |
| $\mu\mu\gamma$ backgrounds | 0.01 |
| Total syst uncertainty | 0.10 |

TABLE I. Summary of systematic errors.

Summarizing, the CLEO Collaboration has obtained a sample of roughly 2000 events of the type $\tau^+\tau^- \to (\pi^+\overline{\nu})(\pi^-\nu)$ taken at $\sqrt{s} \sim 10.6$ GeV. From these the correlation between the energies of the pions has been used to extract the magnitude of the helicity of the tau neutrino. Given that this helicity is known to be negative [4], the result is $h_\nu = -0.99 \pm 0.06 \pm 0.10$. This is consistent with the $V-A$ nature of the charged weak current mediating $\tau$ decay with other measures of the $\nu_\tau$ helicity. [2,3]

We gratefully acknowledge the effort of the CESR staff in providing us with excellent luminosity and running conditions. This work was supported by the National Science Foundation, the U.S. Dept. of Energy, the Heisenberg Foundation, the SSC Fellowship program of TNRLC, Natural Sciences and Engineering Research Council of Canada, and the A.P. Sloan Foundation.

## REFERENCES


[1] The notation in the literature is somewhat confusing in defining the helicity of a fermion such as a neutrino. We use the convention that $h = \vec{s} \cdot \vec{p}/sp$, such that $-1 < h < 1$.

[2] C. Hast, "Selected ARGUS Results on $\tau$-physics", XXIX Recontres de Moriond, March 1994. Their preliminary value is $|h_\nu| = 0.98 \pm 0.04 \pm 0.03$.

[3] D. Buskulic *et al.* (ALEPH Collaboration), Phys. Lett. **B321**, 168 (1994). Their combined analyses yield $|h_\nu| = 0.99 \pm 0.07 \pm 0.04$.

[4] H. Albrecht *et al.* (ARGUS Collaboration), Phys. Lett. **B250**, 164 (1990); H. Albrecht *et al.* (ARGUS Collaboration), Z. Phys. **C58**, 61 (1993). The signed result is $h_\nu = -1.25 \pm 0.23 \,^{+0.15}_{-0.08}$.

[5] J.H. Kühn and F. Wagner, Nuclear Physics **B236**, 16 (1984).

[6] C. Nelson, Physical Review **D43**, 1465 (1991).

[7] W. Fetscher, Physical Review **D42**, 1544 (1990).

[8] Y. Kubota *et al.*, Nucl. Instr. & Method **A320**, 66 (1992).

[9] C. Bebek *et al.*, Nucl. Instr. & Method **A302**, 261 (1991).

[10] S. Jadach and Z. Was, Comp. Phys. Comm. 36, 191 (1985); *ibid.* 64, 267 (1991); S. Jadach, J.H. Kühn, and Z. Was, *ibid.* 64, 275 (1991).

[11] R. Brun *et al.*, CERN Report No. CERN-DD/EE/84-1, 1987 (unpublished).

[12] This form is *exact* for the four final states involving only charged hadrons. For the final state $(\pi\nu)(\mu\nu\overline{\nu})$ the expression has negligible corrections near $h_\nu = -1$.

[13] Particle Data Group, *Review of Particle Properties*, Phys. Rev. **D45**, Part 2 (1992).

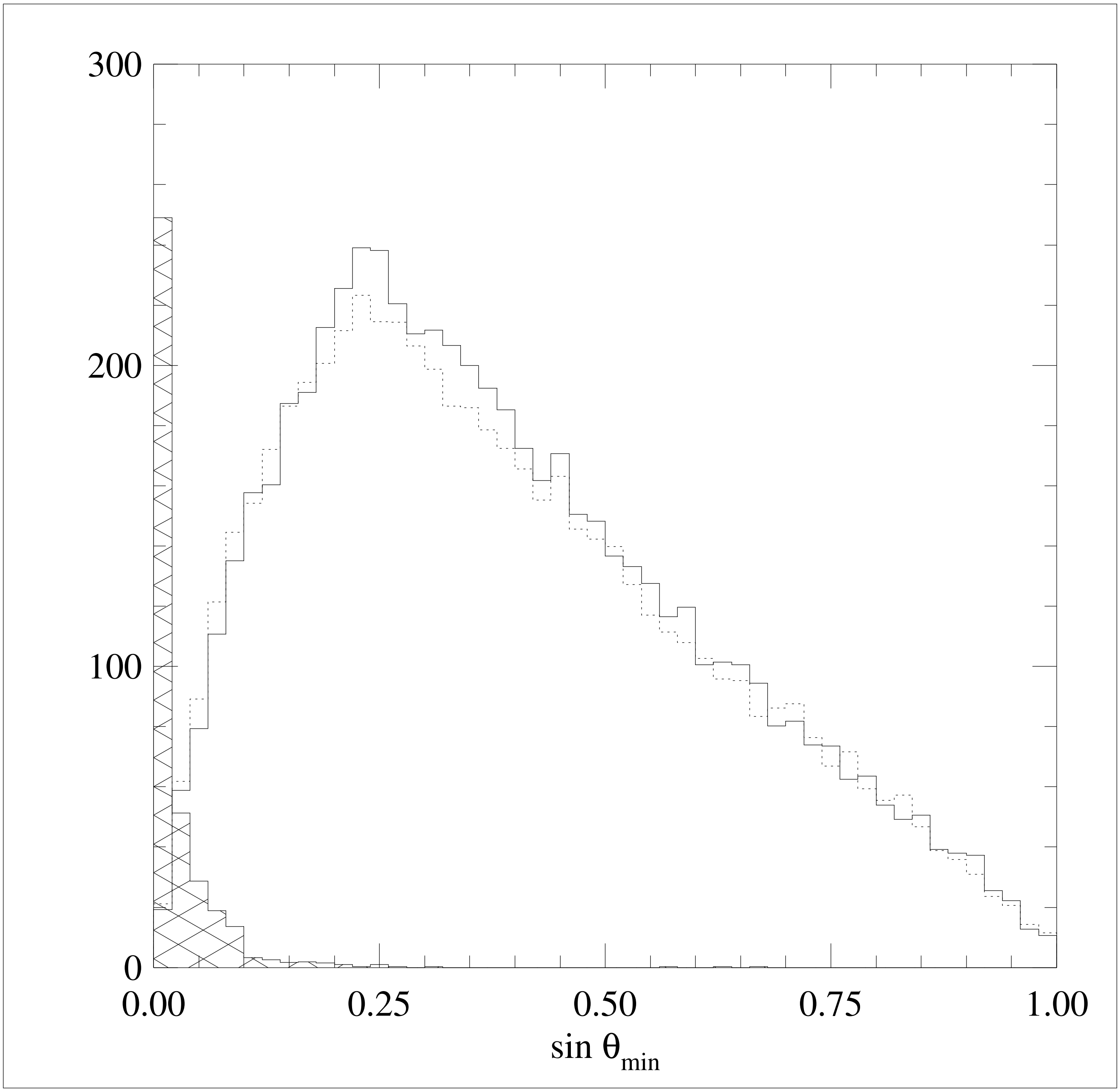


FIG. 1. Distribution from Monte Carlo simulations for the variable sin$\theta_{min}$. The solid and dashed histograms are for $\tau^+\tau^- \rightarrow (\pi^+\overline{\nu})(\pi^-\nu)$ under the assumptions of $V-A$ and $V$, respectively. The hatched histogram is for two-photon production of the final states $e^+e^-\pi^+\pi^-$ and $e^+e^-K^+K^-$.

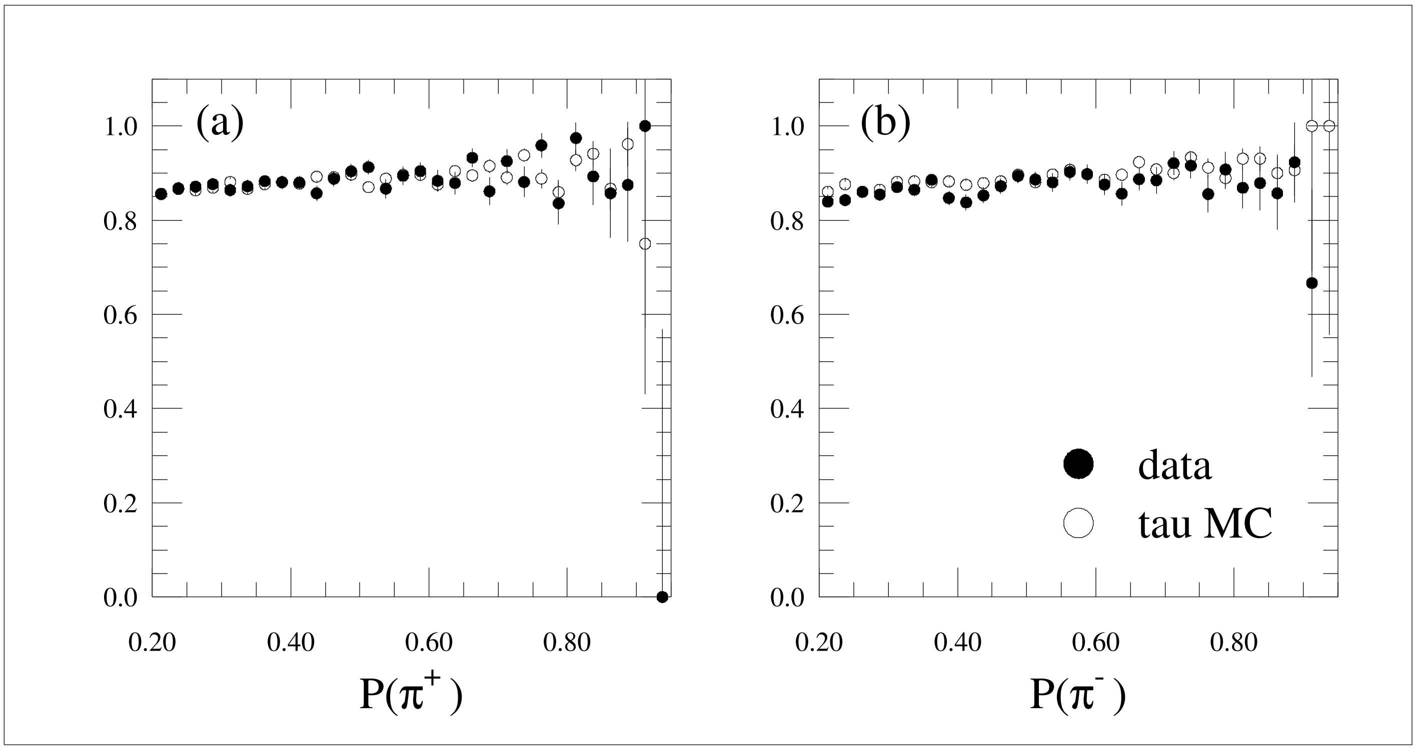


FIG. 2. Fraction of events with no isolated showers versus pion momentum for lepton-vs-$\rho$ events. Solid dots are data and open dots are generic tau Monte Carlo. Showers from pairs which are within $\pm 10\sigma$ of the $\pi^0$ mass are not counted.

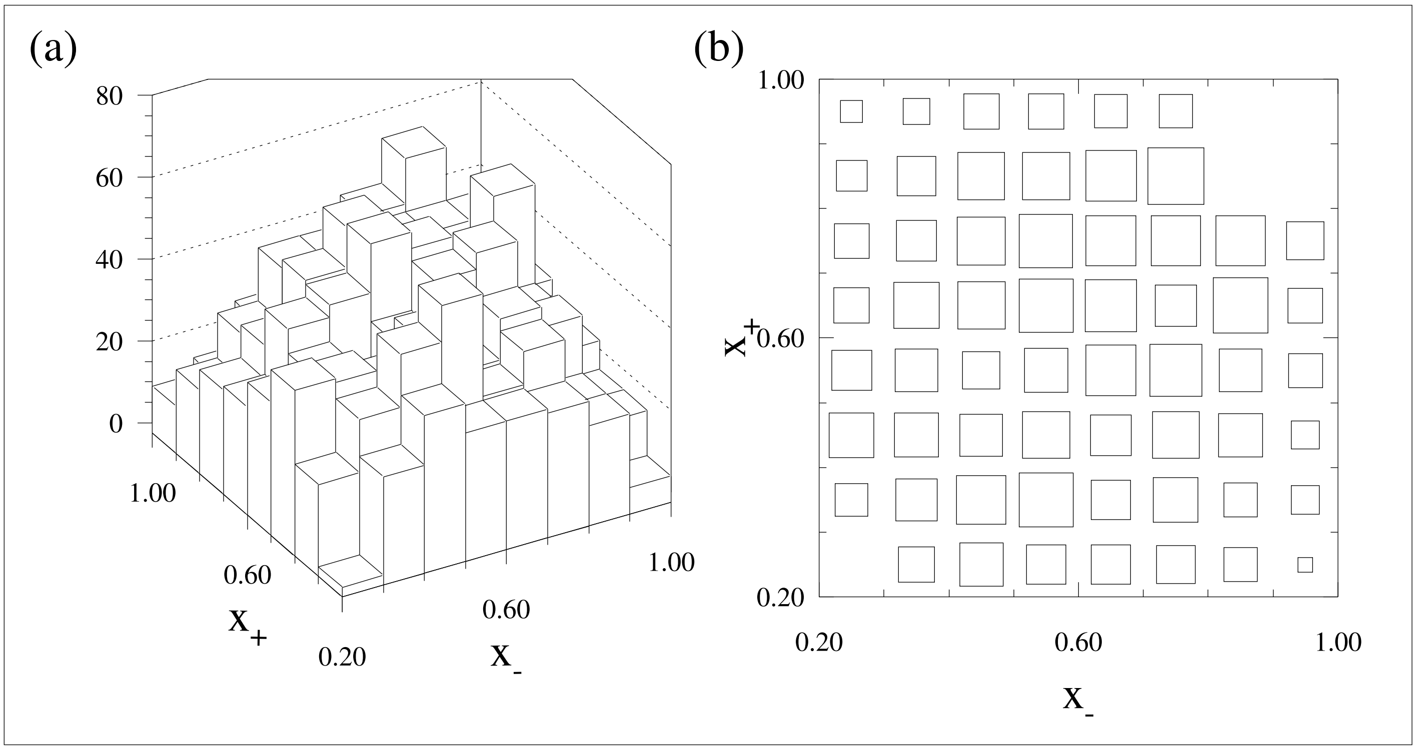


FIG. 3. The $x_+$, $x_-$ distribution for data.

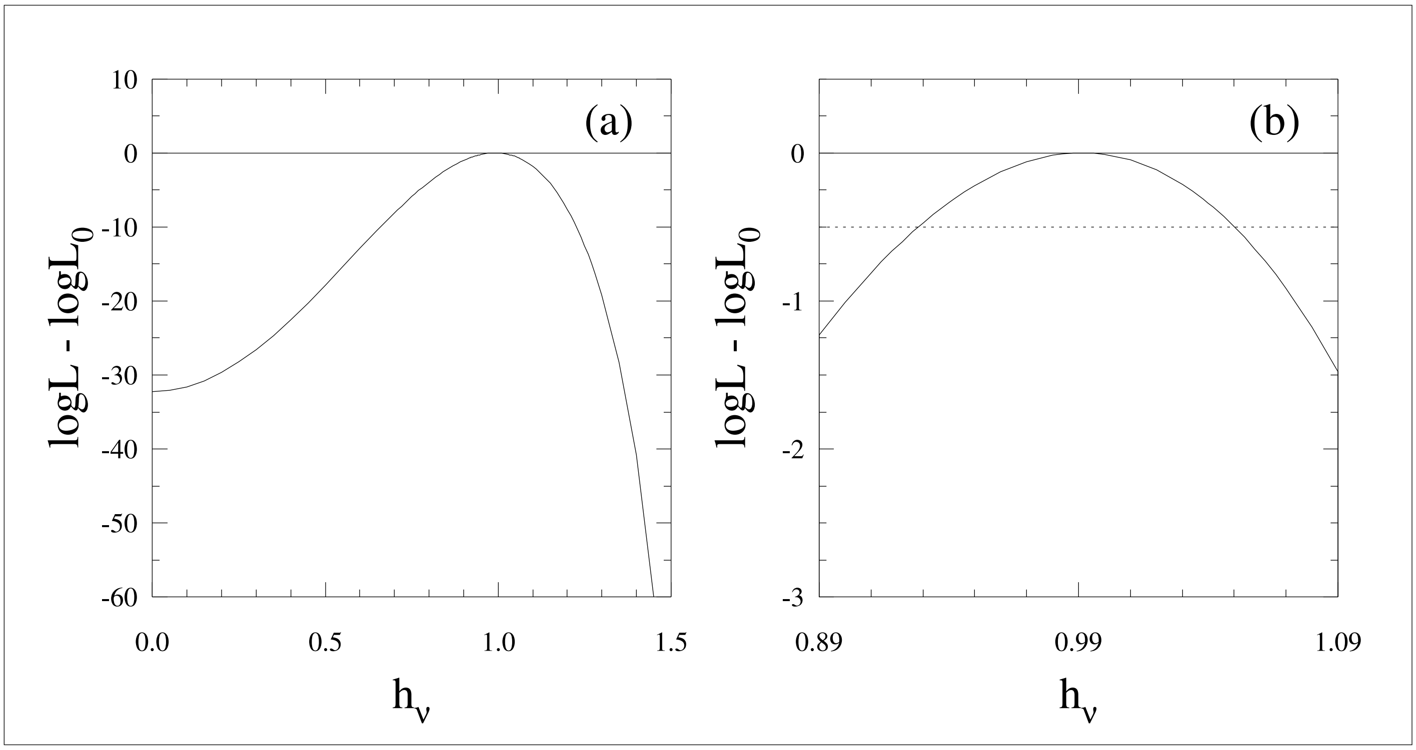


FIG. 4. Log likelihood vs $\xi$ for data. Fig (b) shows an expanded view of the region near the maximum.

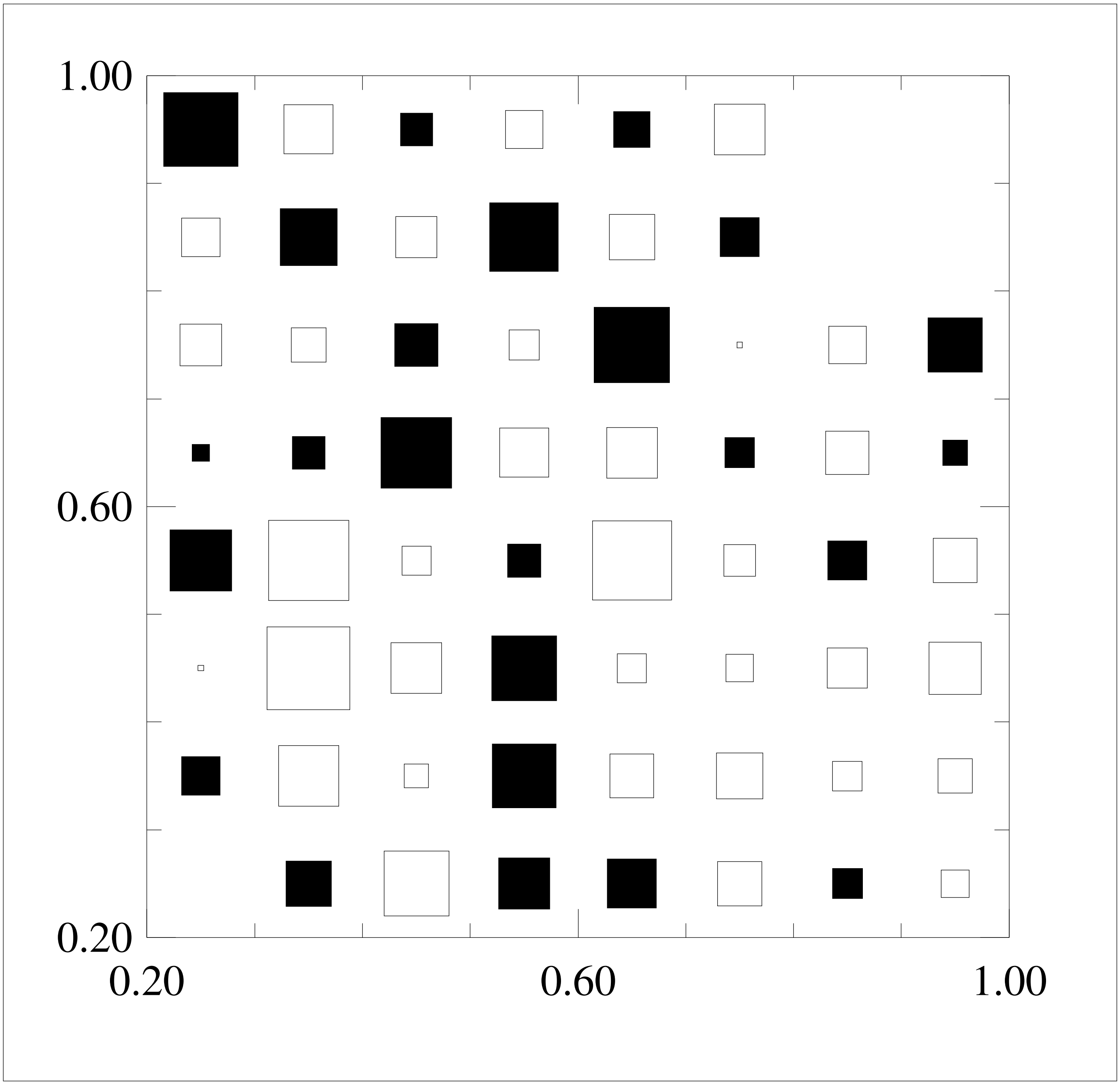


FIG. 5. Distribution of $\Delta_{ij} = (d_{ij} - n_{ij})/{n_{ij}}^{1/2}$ across the $x_+$ versus $x_-$ plane for the best fit value of $h_\nu$. White boxes denote positive values and black boxes, negative.

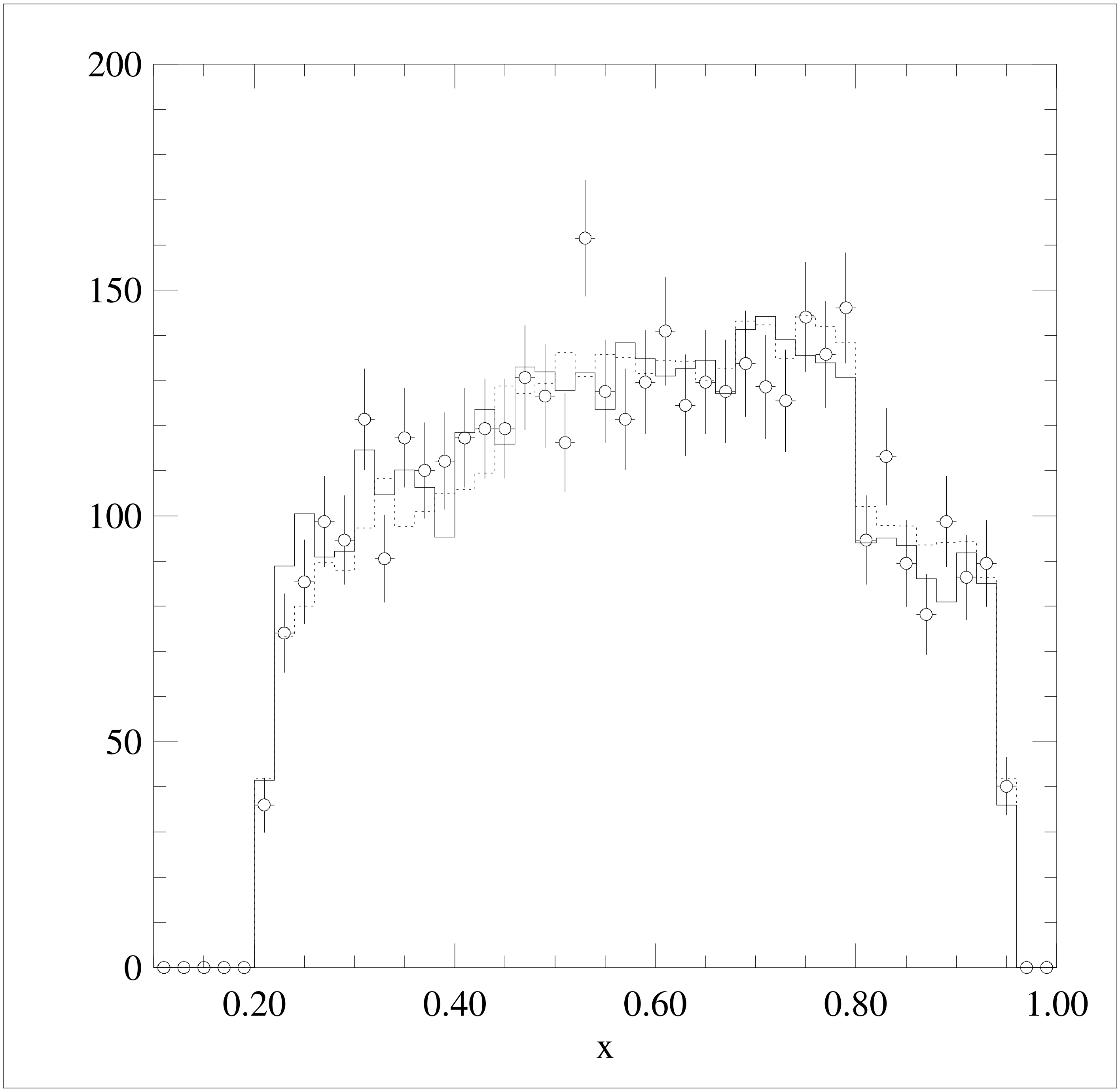


FIG. 6. Spectra of $x$ for both charges for the data (circles) and simulations. The solid histogram is for all $\tau$ decays and the dashed histogram is from the large sample of $\pi\pi$ and $\pi K$ final states produced under $V - A$.